Modeling UpLink Power Control with Outage Probabilities

Kenneth L. Clarkson* K. Georg Hampel† John D. Hobby‡

June 20, 2007

Abstract

We investigate models for uplink interference in wireless systems. Our models account for the effects of outage probabilities. Such an accounting requires a nonlinear, even nonconvex model, since increasing interference at the receiving base station increases both mobile transmit power *and* outage probability, and this results in a complex interaction. Our system model always has at least one solution, a fixed point, and it is provably unique under certain reasonable conditions. Our main purpose is to model real wireless systems as accurately as possible, and so we test our models on realistic scenarios using data from a sophisticated simulator. Our algorithm for finding a fixed point works very well on such scenarios, and is guaranteed to find the fixed point when we can prove it is unique. A slightly simplified model reduces the main data structure for a K-sector market to $16K^2$ bytes of memory.

1 Introduction

While many factors can cause problems for a cell phone call, and many design goals must be balanced in designing a cell phone system, the power used by the phone (the "mobile") is particularly important: this power is limited, and the less it is used, the longer the mobile battery will last and the smaller it can be. Moreover, in a spread spectrum system, the signal from each mobile can interfere with the signal from every other mobile. This motivates the use of sophisticated power control methods: by a variety of means, the system determines how much power is needed by a mobile to carry its call, and the mobile transmits using just that much power. Part of this determination is done at the base stations interacting with the mobile. The result is a complex dynamical system, as mobiles move, signal losses vary, and calls begin and end.

*IBM Research; work was done at Bell Labs
†Bell Labs, Alcatel-Lucent
‡Bell Labs, Alcatel-Lucent

We describe here a computational model of spread-spectrum uplink power control. The model is used within Alcatel-Lucent's Ocelot software for wireless optimization, which handles for example CDMA2000 and UMTS voice and circuit data services. With this application in mind, the model has several properties:

- It models existing wireless systems: it is not a proposal for a new power control system;
- It is designed to be qualitatively accurate over a wide range of conditions, including reverse-link-limited settings;
- It can be evaluated with reasonable speed;
- It is a differentiable function of relevant parameters, and the derivatives can be evaluated with reasonable speed;

The first property implies that we cannot, for example, simply insist of the wireless system that no calls are dropped; such a requirement corresponds to the inclusion of an upper bound on mobile power as a constraint in an optimization problem [1].

We focus here mainly on voice, not data, but some parts of our modeling apply to certain kinds of circuit data services.

Our basic setting is as follows (see for example Lee and Miller [2]). In a given region, there are K base-station antennas (hereafter "sectors"), and a given sector k, with $1 \leq k \leq K$, receives total radio power x_k, from mobiles in the region and from thermal noise and external radio interference sources. Based on the frame error rate, the sector determines a target SIR (signal-to-interference ratio) ϕ_k such that if the signal power received from a mobile is at least $\phi_k x_k$, then the error rate for the mobile will be acceptably low. For each mobile m in soft handoff with the sector, the sector determines the received power s_m, and sends a *power control bit* to the mobile, whose value depends on whether $s_m > \phi_k x_k$, and tells the mobile to increment or decrement its transmit power accordingly. The mobile looks at all such power control bits, and decrements its power if any of the bits suggest it. This protocol keeps the mobile power near the smallest possible such that some sector will receive it with adequate SIR.

Suppose each mobile m is transmitting with power s_m, and is received at sector k with power s_m/L_{km}, where L_{km} is the pathloss factor for the signal traveling from m to k. Let $k(m)$ denote the sector that is currently determining the power transmitted by m, and S_k denotes the set of mobiles m such that $k = k(m)$. Then the power transmitted by $m \in S_k$ is

$$s_m := \phi_k x_k L_{km}, \tag{1}$$

and so for each k',

$$x_{k'} = \eta_{k'} + \sum_k \sum_{m \in S_k} L_{km} \phi_k x_k / L_{k'm},$$

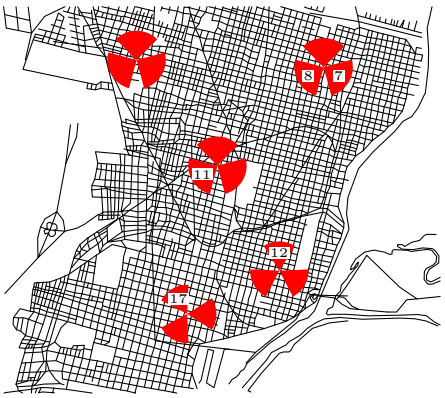

Figure 1: A typical test scenario with some of the sectors labelled with their indices k.

where $\eta_{k'}$ is the power of the noise plus external interference received by sector k'. This equation is correct only under some approximations and assumptions, but it suggests something of the nature of the model that must be evaluated. Put another way, the vector of total radio powers x satisfies the fixed point condition $x = \eta + Ax$, where

$$A_{k'k} := \sum_{m \in S_k} \frac{L_{km}\phi_k}{L_{k'm}}. \tag{2}$$

Note that A is a nonnegative matrix, that is, all its entries are nonnegative. If $\eta = 0$, then $x = Ax$, and x is an eigenvector of the nonnegative matrix A.

The eigenvalues and eigenvectors of nonnegative matrices are well-studied, as the *Perron-Frobenius* theory, and that theory has been applied to the understanding of power control [3]. However, the presence of noise and external interference, implying $\eta > 0$, means that such theory does not directly give the most detailed understanding of power control.

A further complication is reverse-link outage: a call may be dropped if the mobile cannot transmit the target power $\phi_k x_k L_{km}$ as in (1); thus the power s_m is not a linear function of x_k, but instead a sawtooth: at a certain x_k threshold, it goes to zero.

Another complication is *noise rise limitation*: a sector may block calls if the total radio power it receives is above a pre-set threshold. Such a limitation is discussed in Section 5.

A dynamic model of power control might maintain a collection of active mobiles, adding some as calls arrive and dropping others either as normal call termination, or as outages, the result of reverse-link failure. Simulation over time would then yield outage probabilities, average values for the x_k, and so on. However, such a scheme would be too slow for our optimization application, and also, not smooth enough. We use instead a static framework: a (large)

discrete set of locations is fixed, each of which has an estimated probability of being the location of a transmitting mobile. The locations and probabilities are determined elsewhere, and are based on input by the Ocelot user, from a variety of sources, and also on estimates of forward-link coverage probability, and other considerations. The locations could just be points on a regular grid, but Ocelot provides many other options.

We thereby model a dynamic set of mobiles simply as the expectation of the mobile power generated at each location. With some abuse of notation, we index the locations with m, and have corresponding losses L_{km}, power levels s_m, and so on. Since we are modeling probabilities and expectations and not specific mobiles, the power s_m need not be a discontinuous sawtooth function of x_k, but instead can drop off smoothly, as an ensemble average. We might base this dropoff on a log-normal probability distribution for shadow fading. Such a model is discussed in Section 2. However, for efficiency reasons, we use spline-based approximations to the mobile response, as discussed in Section 3. This leads to a function $F : \mathcal{R}^K \to \mathcal{R}^K$, which disregarding call dropping would be $F(x) = \eta + Ax$, but instead we have $F(x)_{k'} = \eta_{k'} + \sum_k \tilde{A}_{k'k}(x_k)$, where $\tilde{A}_{k'k}(x_k)$ is a spline function of the sector k interference x_k. This smooth replacement for the sawtooth is not only more plausible as an estimate, but is convenient computationally: with discontinuities, there may not be a solution to the fixed point problem $x = F(x)$; with the smooth version, we are able to show that under some reasonable conditions, a fixed point solution exists. The solution of the fixed point problem is discussed in Section 5.

We also change the model slightly, to save computational resources, by taking advantage of the similarity between the spline functions $\tilde{A}_{k'k}$ and $\tilde{A}_{k''k}$ for sectors $k'' \neq k'$. The idea is that the interference at sector k' due to uplinks to sector k is closely related to the interference at any other sector k'' due to those same uplinks. This refinement is discussed in Section 4.

Here is the outline for the rest of the paper: we begin in Section 2 by explaining the smoothed sawtooth functions and their relationship to log-normal fading. Then Section 3 gives a spline-based approximation that allows contributions for various locations m to be combined and manipulated efficiently, and Section 4 presents a resource-saving refinement. Next, Section 5 presents robust algorithms for finding fixed points and gives appropriate theorems. The Brouwer fixed point theorem guarantees that our system has a solution. Under certain reasonable conditions that make it a contraction we can prove that the solution is unique and our algorithm finds it. Otherwise, we can only prove that the algorithm finds a fixed point if it gets a good enough starting point. The results in Section 6 include discussions of the various models, and tests on realistic scenarios (not just hexagonal grids). Finally, Section 7 presents conclusions.

2 Smoothed sawtooth functions

Consider a single term from the sum (2) as changed to account for the dropping of calls due to reverse-link limitations. If $\hat{s}$ is the maximum mobile uplink

transmit power, multiplying the term by

$$\begin{cases} x_k & \text{if } s_m < \hat{s} \\ 0 & \text{otherwise,} \end{cases}$$

where again $s_m := x_k L_{km} \phi_k$ for $m \in S_k$, gives the sawtooth function that we need to smooth by considering the ensemble average of a dynamic set of mobiles and finding the contribution to interference due to location m. The sawtooth-based interference contribution to sector k' from location m transmitting to location k could thus be expressed as

$$\frac{\hat{s}}{L_{k'm}} \gamma_m Q^-(\gamma_m),$$

where

$$Q^-(t) := \begin{cases} 1 & \text{if } t < 1 \\ 0 & \text{otherwise,} \end{cases}$$

and the ratio $\gamma_m := s_m/\hat{s}$. Another way to describe this is as

$$\frac{\hat{s}}{L_{k'm}} G(\gamma_m),$$

where $G(\gamma)$ is the sawtooth function

$$G(\gamma) := \gamma Q^-(\gamma). \tag{3}$$

Replace pathlosses L_{km} and $L_{k'm}$ by $L_{km} \exp(R_{km})$ and $L_{k'm} \exp(R_{k'm})$, where random variables R_{km} and $R_{k'm}$ are $N(0, \sigma)$, that is, normally distributed with zero mean and standard deviation σ. This implies replacing γ_m by $\gamma_m \exp(R_{km})$ as well. Then the expected interference contribution for location m could be estimated as

$$\begin{aligned} &\mathbf{E}\left[\frac{\hat{s}}{L_{k'm} \exp(R_{k'm})} \gamma_m \exp(R_{km}) Q^-(\gamma_m \exp(R_{km}))\right] \\ &\quad = \frac{\hat{s}\gamma_m}{L_{k'm}} \mathbf{E}\left[\exp(R_{km} - R_{k'm}) Q^-(\gamma_m \exp(R_{km}))\right], \end{aligned} \tag{4}$$

although the non-outage condition $Q^-(\gamma_m \exp(R_{km})) = 1$ might be more generally modeled as a non-outage probability $Q()$.

It may be that R_{km} and $R_{k'm}$ are partially correlated, so we assume that there is some $\beta \in [0, 1]$ and $N(0, \sigma)$-distributed random variable $\hat{R}_{k'm}$, independent of R_{km}, so that $R_{k'm} = (1 - \beta) R_{km} + \beta \hat{R}_{k'm}$, and so

$$\exp(R_{km} - R_{k'm}) = \exp(-\beta \hat{R}_{k'm}) \exp(\beta R_{km}).$$

If we use the latter expression in (4), use the independence of R_{km} and $\hat{R}_{k'm}$, and observe that $\mathbf{E}[\exp(-\beta \hat{R}_{k'm})] = \mathbf{E}[\exp(\beta \hat{R}_{k'm})]$, the expected interference

contribution becomes

$$\frac{\hat{s}\gamma_m}{L_{k'm}}\mathbf{E}\left[\exp(R_{km}-R_{k'm})Q^-(\gamma_m\exp(R_{km}))\right]$$
$$=\frac{\hat{s}\gamma_m}{L_{k'm}}\mathbf{E}[-\beta R_{k'm}]\mathbf{E}\left[\exp(\beta R_{km})Q^-(\gamma_m\exp(R_{km}))\right]. \quad (5)$$

The expectation over R_{km} can be written out as

$$\mathbf{E}\left[\exp(\beta R_{km})Q^-(\gamma_m\exp(R_{km}))\right]$$
$$=\frac{1}{\sqrt{2\pi}}\int_{-\infty}^{\infty}\exp(-t^2/2)\exp(\beta t\sigma)Q^-(\gamma_m\exp(t\sigma))\,dt.$$

Note that $Q^-(\gamma_m\exp(t\sigma))=1$ only when $\ln(\gamma_m)+t\sigma<0$ or equivalently, $t<-\ln(\gamma_m)/\sigma$. Furthermore,

$$\exp(-t^2/2)\exp(\beta t\sigma)=\exp(\beta^2\sigma^2/2)\exp(-(t-\beta\sigma)^2/2),$$

so that the expectation over R_{km} becomes

$$\mathbf{E}\left[\exp(\beta R_{km})Q^-(\gamma_m\exp(R_{km}))\right]$$
$$=\frac{\exp(\beta^2\sigma^2/2)}{\sqrt{2\pi}}\int_{-\infty}^{-\ln(\gamma_m)/\sigma}\exp(-(t-\beta\sigma)^2/2)\,dt$$
$$=\frac{\exp(\beta^2\sigma^2/2)}{\sqrt{2\pi}}\int_{-\infty}^{-\ln(\gamma_m)/\sigma-\beta\sigma}\exp(-u^2/2)\,du.$$
$$=\exp(\beta^2\sigma^2/2)\Phi[-\ln(\gamma_m)/\sigma-\beta\sigma],$$

where $\Phi(x)$ is the normal cumulative distribution function at x, the probability that a $N(0,1)$ random variable is less than x.

Finally, substituting the above expression into (5), and also substituting $\exp(\beta^2\sigma^2/2)=\mathbf{E}[\exp(\beta\hat{R}_{k'm})]$, gives the following expression for the expected interference contribution

$$\frac{\hat{s}\,\exp(\beta^2\sigma^2)}{L_{k'm}}\gamma_m\Phi[-\ln(\gamma_m)/\sigma-\beta\sigma]. \quad (6)$$

Note that $\gamma_m\Phi[-\ln(\gamma_m)/\sigma-\beta\sigma]$ is essentially a smoothed version of (3).

3 Spline Approximations

The normal CDF needed for (6) is easily evaluated via the error function erf(), since $2\Phi(x)=1+\mathrm{erf}(x/\sqrt{2})$. However, although erf() can be found in any good mathematical subroutine library, it would be awkward to handle sums of such interference contributions for many different locations $m\in S_k$. Viewing (6) as a function of x_k rather than γ_m requires a substitution

$$\gamma_m=\frac{s_m}{\hat{s}}=\frac{\phi_k x_k L_{km}}{\hat{s}}$$

that shifts the x_k values at which (6) begins to fall to zero. Even if we were to scale them so that their initial slopes match, the functions (6) for different locations m would be as in Figure 2a.

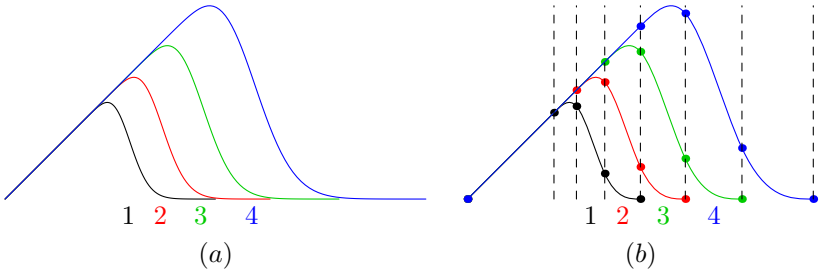

Figure 2: (a) smoothed sawtooth functions for various locations m where γ_m/x_k differs by factors of $\alpha = 1.26$; (b) the corresponding spline approximations with dashed lines at the ends of spline segments.

Spline approximations such as those shown in Figure 2b are much more convenient when taking smoothed sawtooth functions for various locations m, and adding them up in a manner analogous to (2). The splines are piecewise-cubic polynomial functions chosen to have second-order continuity at the *knots* where one cubic polynomial segment joins the next one. Placing the knots at powers of a parameter α ensures that any linear combination of these spline functions will be a piecewise cubic spline with the same knot spacing.

The smoothed sawtooth spline is conveniently represented by a Beziér control polygon as shown in Figure 3. It consists of a straight line joining the origin to a point (x_0, a_0) followed by three curved segments, followed by a horizontal straight line beginning at (x_3, a_9). The value of the spline function at $x_i + t(x_{i+1} - x_i)$ for $0 \le i < 3$ and $0 \le t \le 1$ is

$$(1-t)^3 a_{3i} + 3t(1-t)^2 a_{3i+1} + 3t^2(1-t)a_{3i+2} + t^3 a_{3i+3}. \tag{7}$$

The second-order continuity conditions determine $a_0, a_1, \ldots, a_9$ via 10 linear equations in 10 unknowns:

$$\begin{aligned} a_i &= 1 + (\alpha - 1)i/3 && \text{for } i < 3 \\ \alpha(a_i - a_{i-1}) &= a_{i+1} - a_i && \text{for } i = 3, 6 \\ \alpha^2(a_i - 2a_{i-1} + a_{i-2}) &= a_i - 2a_{i+1} - a_{i+2} && \text{for } i = 3, 6 \\ a_i &= 0 && \text{for } i > 6 \end{aligned} \tag{8}$$

For any fixed α, (7) and (8) determine a function of x that we shall call $G_\alpha(x)$. It has been normalized to have initial slope 1 because it is now inconvenient to include factors from (6) such as $\gamma_m \hat{s}/L_{k'm}$.

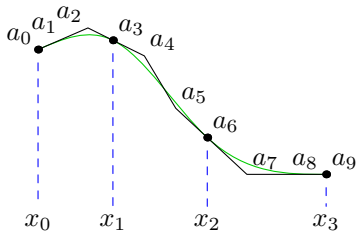

Figure 3: The Beziér control polygon for the curved part of a smoothed sawtooth spline.

The complete set of normalized smoothed sawtooth splines is

$$\left\{ \frac{G_\alpha(b\alpha^i x)}{b\alpha^i} \;\middle|\; i \in \mathbf{Z} \right\},$$

where b is a bias parameter to be chosen along with α. We must choose α and b so that

$$\frac{G_\alpha(b\gamma)}{b} \approx \gamma\Phi[-\ln(\gamma)/\sigma - \beta\sigma] \tag{9}$$

as functions of γ.

It is enough to consider $\beta = 0$, since the effect of β can be accounted for by scaling b: if (9) holds with $\beta = 0$ and at $\gamma' := \gamma\exp(\beta\sigma^2)$, then for $b' := b\exp(\beta\sigma^2)$,

$$\begin{aligned} \frac{G_\alpha(b'\gamma)}{b'} &= \exp(-\beta\sigma^2)\frac{G_\alpha(b\gamma')}{b} \\ &\approx \exp(-\beta\sigma^2)\gamma'\Phi[-\ln(\gamma')/\sigma] \\ &= \gamma\Phi[-\ln(\gamma)/\sigma - \beta/\sigma]. \end{aligned}$$

We can quantify the difference between the two functions by evaluating each side of (9) at

$$\gamma_m = \sigma^{-3.00}, \sigma^{-2.97}, \sigma^{-2.94}, \ldots, \sigma^{3.00}$$

and taking the RMS mean of the differences. For any given σ, it is easy to choose α and b so as to minimize this. For example, exhaustively trying multiples for 0.0001 for α and b gives the results in Table 1. If it is more convenient to have an empirical formula based on this table, choose

$$L = 2.043\sigma + .5625\sigma^2$$

and then let

$$\alpha = e^L$$

and

$$b = \frac{(0.1127 + 0.3355\alpha + 0.451\alpha^2 + 0.00041\alpha^3)\exp(\beta\sigma^2)}{1 + 0.0042\alpha}.$$

Table 1: Choosing α and b so as to satisfy (9)

σ	$\ln \alpha$	b	RMS error
0.09212	0.1799	1.14574	0.00379052
0.2303	0.457	1.76343	0.00498369
0.4606	0.9679	4.09981	0.00748236
0.6909	1.5904	12.3288	0.00915151
0.9212	2.3385	50.1016	0.0108936
1.1515	3.1548	239.085	0.0173641
1.3818	3.9875	1140.56	0.030776
1.6121	4.8184	5061.15	0.0540373
1.8424	5.668	21703.5	0.0943915
2.0727	6.6114	141023	0.165292

Note that we have included the $\exp(\beta\sigma^2)$ that accounts for $\beta \neq 0$.

These smoothed sawtooth splines need to be added up for all locations m served by sector k so as to obtain a function $\bar{A}_{k'k}$ for interference at sector k' due to mobiles owned by sector k as a function of x_k, the interference at sector k. In other words, we need a spline-based generalization of (2). For each m, we must choose a smoothed sawtooth spline

$$\frac{G_\alpha(b\alpha^{i_m} x_k)}{b\alpha^{i_m}}$$

so that $\alpha^{i_m} x_k \approx \gamma_m$, or perhaps use

$$(1-\xi_m) G_{\alpha,i_m,b}(x_k) + \xi_m G_{\alpha,i_m+1,b}(x_k)$$

where $((1-\xi_m)\alpha^{i_m} + \xi_m \alpha^{i_m+1})x_k = \gamma_m$. Then multiply by the

$$\frac{\hat{s}\, \exp(\beta^2\sigma^2)}{L_{k'm}}$$

factor of (6).

$$\bar{A}_{k'k}(x_k) = \sum_{m \in S_k} \frac{\hat{s}\, \exp(\beta^2\sigma^2)}{L_{k'm}} \left[(1-\xi_m) frac G_\alpha(b\alpha^{i_m} x_k) b\alpha^{i_m}(x_k) + \xi_m frac G_\alpha(b\alpha^{i_m+1} x_k) b\alpha^{i_m} \right].$$

4 Using Similarity to Save Resources

Since the path loss L_{km} can vary by more than a factor of 1000 as the location m ranges over S_k, the $\bar{A}_{k'k}$ function will typically have dozens of spline segments. This seems like a lot of information to store and manipulate for each pair of sectors $k'k$, especially since $\bar{A}_{k'k}$ functions for a common k but differing k' tend to be related, as shown in Figure 4.

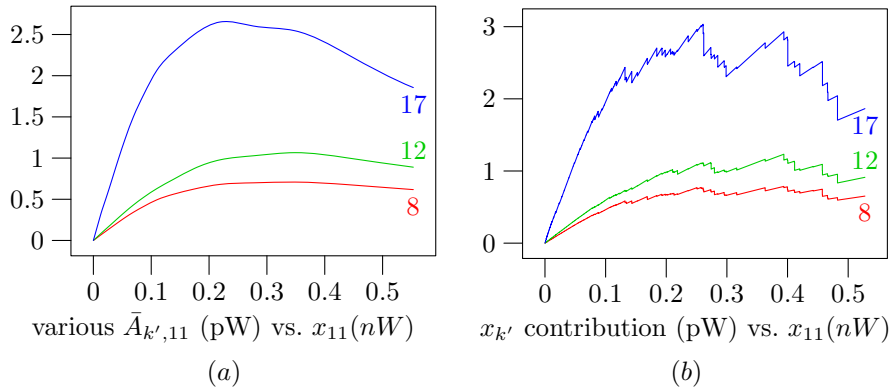

Figure 4: (a) $\bar{A}_{k'k}$ functions for $k = 11$ and various k'; (b) the corresponding functions based on raw unsmoothed sawteeth. The test data are from the scenario shown in Figure 1.

Since the knots are all aligned, it is easy to add up the the spline functions $\bar{A}_{k'k}$ to obtain a master spline function

$$A_k(x) = \frac{\sum_{k'} \bar{A}_{k'k}(x)}{\sum_{k'} \bar{A}'_{k'k}(0)}$$

that can be thought of as an average $\bar{A}_{k'k}$, normalized to have unit initial slope.

The resource-saving idea is to store K master spline functions and K^2 simple transformations instead of K^2 spline functions. If the simple transform is just to scale $\bar{A}_k$ to have the right initial slope, the result is as shown in Figure 5a. Since the dashed lines for the scaled versions of $\bar{A}_k$ are sometimes far from the corresponding solid curves $\bar{A}_{k'k}$, the transformation that just scales by $A'_{k'k}(0)$ appears to be too simple.

The more promising transformation illustrated in Figure 5b is to use

$$\tau_{k'k} x \left(\frac{\bar{A}_k(x)}{x} \right)^{\bar{\tau}_{k'k}} \tag{10}$$

in place of $\bar{A}_{k'k}(x)$, where $\tau_{k'k}$ and $\bar{\tau}_{k'k}$ are chosen based on $\bar{A}'_{k'k}(0)$ and $\bar{A}_{k'k}(\bar{x})$ for some fixed $\bar{x}$ that can be thought of as an a priori guess at a typical interference level. This way, there are just two values to keep track of for each $k'k$ pair while we consider various locations m. After finding these $2K^2$ values and the K master spline functions $\bar{A}_k$, we can set

$$\tau_{k'k} = \bar{A}'_{k'k}(0) \quad \text{and} \quad \bar{\tau}_{k'k} = \frac{\log(\bar{A}_{k'k}(\bar{x})/(\tau_{k'k}\bar{x}))}{\log(\bar{A}_k(\bar{x})/\bar{x})}$$

for each pair $k'k$. (In practice, one must impose also a positive lower bound on $\bar{\tau}_{k'k}$ to avoid 0^0 in (10).)

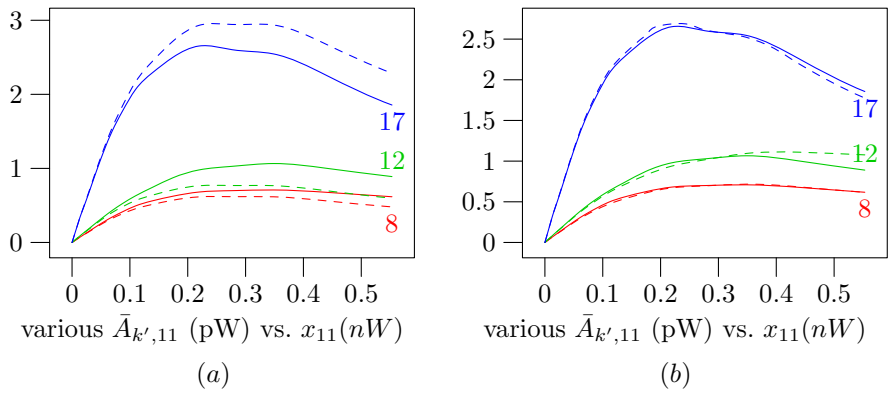

Figure 5: (a) $\bar{A}_{k'k}$ functions for $k = 11$ (solid) versus transforming $\bar{A}_k$ to match initial slope (dashed); (b) same except dashed lines are $\bar{A}_k$ transformed to match initial slope, and value at 0.3nW.

5 Finding a Fixed Point

The last three sections have described different versions of a function that gives the (expected) interference received at sector k' from mobiles whose primary sector is k. These are:

1. A linear function equal to zero at zero;
2. A sum of sawtooth functions;
3. A sum of smoothed sawteeth, based on lognormal shadow fading, as discussed in Section 2;
4. A sum of spline functions, that can be viewed as approximations to the smoothed sawteeth, as in § 3;
5. For sector k', a function that is a transformed version, of a "master" spline function $\bar{A}_k$ for sector k, as in § 4.

In whatever way each such function $A_{k'k}(x_k)$ is defined, the result is an estimate $\eta_{k'} + \sum_k A_{k'k}(x_k)$ of the interference received at sector k'. This could also be written as a vector $\eta + \bar{F}(x_k)\mathbf{1}$, where $\bar{F}(x_k)$ is a $K \times K$ matrix with $\bar{F}(x_k)_{k'k} = A_{k'k}(x_k)$, and $\mathbf{1}$ is the K-vector of all ones. Defining the function $F : \mathcal{R}^K \to \mathcal{R}^K$ by $F(x) = \eta + \bar{F}(x)\mathbf{1}$, the interference vector thus obeys the condition $x = F(x)$. In other words, it is a fixed point of the mapping F.

When the sector-to-sector interference function is linear, as listed first above, the $\bar{F}$ function returns a real matrix, and the fixed point problem is to solve a linear system $x = \eta + Ax$. For the second model listed, a sum of sawteeth, the corresponding fixed-point problem may be unsolvable due to discontinuities. The smoothed version given third is not computationally convenient, as discussed. It remains to consider finding fixed points for the last two versions,

with spline-based functions, and with the more compact spline-based scheme of Section 4.

Before discussing methods of solution of such general fixed point problems, we consider the implementation of a model of *noise-rise limits* for power control. Here sector k tries to keep $x_k \le \hat{\rho}\eta_k$, for some $\hat{\rho} > 1$, by blocking calls if necessary. The simplest way to model this is just to compose F with a function that limits the kth component to at most $\hat{\rho}\eta_k$(perhaps with some kind of smoothing to account for x_k being an expectation and the sector not being able to measure x_k or η_k precisely).

A more sophisticated model of noise rise limitation accounts for sector k's decision to drop calls also reducing its contributions to $x_{k'}$ for all $k' \neq k$: replace $\mathbf{1}$ in $\eta + \bar{F}(x)\mathbf{1}$ with a vector whose kth component is a probability that sector k decides not to block a call due to noise rise concerns. In other words,

$$F(x) = \eta + \bar{F}(x)h(x), \quad \text{where } h(x)_k = \begin{cases} 1 & \text{if } x_k \ll \hat{\rho}\eta_k; \\ 0 & \text{if } x_k \gg \hat{\rho}\eta_k. \end{cases}$$

By any of these definitions, F is a smooth function that maps the positive orthant into a rectilinear region

$$U = \{x \in \mathcal{R}^K \mid \eta_k \le x_k \le \mu_k\},$$

where the upper bound μ_k can come from the noise rise limitation or from the fact that each component of $\bar{F}$ is a univariate function that has a finite maximum on $[0, \infty)$ because it is a sum of G_α functions that have this property (see Figure 2), and the transformation (10) preserves this. In other words, we have just defined a point μ such that η and μ are opposite corners of a box U.

Since U is homeomorphic to a closed ball and the continuous function F maps the whole positive orthant (a superset of U) into U, the Brouwer fixed point theorem guarantees that there is at least one fixed point $x = F(x)$. (Note that the theorem does not require F to be bijective or surjective.)

It would also be desirable to guarantee a unique fixed point and provide an algorithm that finds it efficiently. A popular approach used by Yates [4] and others is to let the algorithm be Picard iteration, where repeatedly $x \leftarrow F(x)$, and also to give conditions under which Picard iteration provably converges to a unique fixed point. For example, if we can exhibit a real number $\kappa < 1$ and a vector norm $\|\cdot\|_*$ under which

$$\|F(x) - F(y)\|_* \le \kappa \|x - y\|_* \quad \text{for all } x, y \in U, \tag{11}$$

then the fixed point is unique and Picard iteration converges from any starting point in U. Nuzman [5] has shown that this type of argument can be applied to non-monotonic functions that resemble F, but the spline functions on which F is based provide too much freedom to allow for much hope of a general theorem of this type.

In order to have an algorithm that is as reliable as possible, we certainly need guaranteed convergence if (11) holds. We can do this by producing a sequence

of iterates $x^{(1)}, x^{(2)}, x^{(3)}, \ldots$, where each

$$\left\|x^{(i+1)} - F(x^{(i+1)})\right\| \leq \kappa \left\|x^{(i)} - F(x^{(i)})\right\| \tag{12}$$

for the standard Euclidean norm. Such a sequence clearly converges to a fixed point, and Picard iteration under (11) provides one way to achieve it if we assume that $\|\cdot\|_*$ is sufficiently similar to the Euclidean norm. The idea is that a few iterations, each of which reduces $\|x - F(x)\|_*$ by the factor κ should suffice to reduce $\|x - F(x)\|$ by that factor.

Another way to find a fixed point is to use Newton iteration to look for a zero of $F(x) - x$. Such an iteration does not require (11) and is known to converge quadratically if the initial x is sufficiently close to a solution of $F(x) - x = 0$, except there is no good way to know a priori what is "sufficiently close." This suggests a hybrid algorithm that uses an intelligent starting point, does Newton iterations, but switches to Picard iterations if necessary to obey (12).

1. Use binary search to find a point x on the line between η and μ where the number of negative components in $x - F(x)$ is between $\frac{1}{3}K - \frac{1}{2}$ and $\frac{2}{3}K + \frac{1}{2}$.

2. Compute a Newton step $\Delta x = (J_F(x) - I)^{-1}(F(x) - x)$ and find the maximum $\bar{\lambda}$ such that $x - \bar{\lambda}\Delta x \in U$. Here $J_F(x)$ is the Jacobian of F.

3. Let $y = x$, $e_0 = \|x - F(x)\|$ and exit if e_0 is tiny. Then if $\bar{\lambda} < 0.8$, do Picard iterations and go to Step 2 as soon as $\|x - F(x)\| \leq \kappa e_0$.

4. Let $\hat{\lambda} = \max(\bar{\lambda}, 1 + 10^{-6})$ and $\lambda = \min(1, \bar{\lambda})$. While $\|x - F(x)\| > e_0$ for $x = y - \lambda\Delta x$, iterate $\lambda \leftarrow \max(\lambda/2, 2\lambda - \hat{\lambda})$.

5. If $\|x - F(x)\| > \kappa e_0$, do Picard iterations until $\|x - F(x)\| \leq \kappa e_0$. Then go to Step 2

For each i, the ith iteration of Steps 2–5 advances from $x^{(i)}$ to $x^{(i+1)}$ while trying to ensure that the condition of (12) is satisfied. The testing of λ values less than one, if one Newton step is not feasible or does not help, is a *line search* along the Newton step direction. The use of $\hat{\lambda}$ in this line search causes it to back off slowly at first if 1 Newton step goes close to the edge of U, something that often turned out to be beneficial in practice

If a Newton step is significantly out of bounds or makes so little progress that $e_0 \geq \|x - F(x)\| > \kappa e_0$, the algorithm resorts to Picard iterations. An excessive number of such iterations in Steps 3 or 5 should be treated as a failure indication.

Of course, the application of $(J_F(x) - I)^{-1}$ is based on LU or LUP factorization and back-substitution, instead of a matrix inversion. Furthermore, the Jacobian $J_F(x)$ often does not change much from one iteration to the next, so it may be possible to avoid an $\Omega(K^3)$ step here by using the factorization for a previous step in an iterative improvement scheme.

6 Results

A version of the algorithm has been tested extensively as part of Alcatel-Lucent's Ocelot software, but it is not practical to rerun it on more than a few test scenarios as shown in Table 2. We will not consider defining the function $F : \mathcal{R}^K \to \mathcal{R}^K$ based on unsmoothed sawtooth functions, because fixed point iteration did not converge for any of the scenarios in Table 2. (It continually jumps back and forth across a particular discontinuity.) This leaves $F(x) = \eta + Ax$, and also the spline based functions, with and without resource-saving transformations, which we shall refer to as F§4 and F§3. Except as stated below, these F functions do not include the noise rise limitation.

Table 2: The test scenarios

Label	K	Explanation
H57	57	Hex pattern with 3 sectors per base station
M39	39	Metro area with population $\approx$ 500 thousand
M39h	39	M39 with 14 times the traffic near Sector 7
M60	60	Metro area with population $\approx$ 700 thousand
M115	115	Metro area with population $\approx$ 2 million

Table 3: Sample results with all powers given in picowatts. For two scenarios, the solution to $x = \eta + Ax$ was not usable because it had some negative entries. The notation "$5+1P$" means that 1 Newton step had to be replaced by a Picard iteration.

	η_k	average x_k			max x_k			Newton steps	
	$\forall k$	$\eta + Ax$	F§3	F§4	$\eta + Ax$	F§3	F§4	F§3	F§4
H57	17.3	19.8	19.4	19.4	20.2	19.7	19.7	4	4
M39	17.3	35.5	23.7	23.5	99.6	31.0	30.6	4	4
M39h	17.3	—	25.1	25.1	—	141	131	$5+1P$	$5+1P$
M60	17.3	23.1	21.6	21.6	60.4	35.6	36.1	4	4
M115	17.3	—	21.3	21.2	—	35.2	33.9	5	6

Table 3 summarizes the results for the three versions of F and the four scenarios. As the table suggests, it is usually easy to solve for $x = F(x)$ under typical scenarios, and very few Newton iterations are needed to achieve full accuracy in 64-bit floating point. The only case where a Newton step failed and Picard iteration was needed was the contrived scenario M37h.

Note that the Brouwer fixed point theorem does not apply to $x = \eta + Ax$ since there is no vector of upper bounds μ in that case. Of course, singularity of the $A - I$ matrix is not a problem in practice, but there was one case where this simple linear system failed to give a reasonable solution. This can happen if entries of A are large enough to allow $\|Ax\| > \|x\|$ for some vectors x.

As can be seen from Table 4, the simple $\eta + Ax$ function gives different (and presumably less accurate) results even when it does yield a reasonable solution. Contrast this with the resource-saving transformations of Section 4 which never had a significant effect on the solution.

Table 4: Relative differences ($\|x - y\| / (\|x\| + \|y\|)$) between solution vectors x and y for each pair of different F definitions.

	$Ax + \eta$ vs. F§3	$Ax + \eta$ vs. F§4	F§3 vs. F§4
H57	0.012	0.012	0.0019
M39	0.29	0.29	0.013
M39h	—	—	0.029
M60	0.090	0.090	0.0036
M115	—	—	0.0065

Only the M39h scenario (a portion of which was shown in Figure 1) had any x_k values large enough to trigger reasonable noise rise limits. As Table 5 suggests, qualitatively similar result were obtained from the simple composition of F with a function that smoothly limits each component to $\hat{\rho}\eta_k$ and from the more complicated scheme $F(x) = \eta + \bar{F}(x)h(x)$.

Table 5: Selected x_k values from the F§4 fixed point for the M39h scenario with various noise rise limitations. All powers are in picowatts and all η_k values were 17.3pW.

	None	Simple $\bar{\rho} = 4.5$	via $F(x)h(x)$ $\bar{\rho} = 4$
7	130.63	65.83	67.16
8	31.60	28.11	26.85
11	21.56	21.29	21.42
12	29.49	26.69	25.55
17	21.29	20.99	21.05

A relatively large amount of smoothing was used so that $1 > h(x_k) > 0$ for $0.8\hat{\rho}\eta_k < x_k < 1.2\hat{\rho}\eta_k < x_k$ and consequently $\hat{\rho}$ had to be reduced slightly in order to make x_7 roughly agree with the result of simple componentwise noise rise limitation. The smoothing is needed since it is difficult to find the fixed point if $h(x_k)$ changes very suddenly. For instance, with $0.96 \ldots 1.04$ instead of $0.8 \ldots 1.2$, a failed Newton step leads to a Picard iteration that also fails. We also tried a more cautious $x \leftarrow (x + F(x))/2$ iteration, but it also fails. As can be seen from Figure 6, the iterates oscillate in 3-cycle instead. A smoother $h(x_k)$ function avoids this, but it may be safer to use the simpler componentwise noise rise limitation instead. Extensive experience with it has not shown any convergence difficulties.

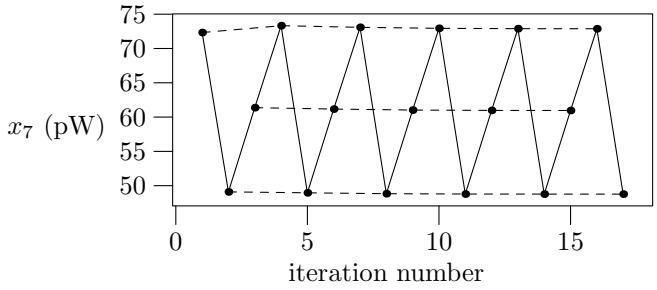

Figure 6: Convergence behavior for the heavily-loaded sector in the M39h scenario. Dashed lines show relationships between the results of every 3rd iteration.

7 Conclusions

We have given realistic models for uplink power control for voice and circuit data services under a variety of technologies. The use of averages and fading probabilities smooths out discontinuities that could otherwise prevent the model from having a solution. Although incorporating outage probability leads to a nonlinear system for which we cannot guarantee convergence, we have ensured that F and its Jacobian are easy to evaluate, and the hybrid algorithm for finding the fixed point has proved to be very reliable in practice.

Without the outage probabilities, one gets a simple $\eta + Ax$ function that often leads to significantly different solution vectors x and sometimes fails to give any reasonable solution. With outage probabilities, we get the F functions from Sections 3 and 4 for which the Brouwer fixed point theorem guarantees the existence of a reasonable solution that satisfies $x = F(x)$.

The F function from Section 4 requires K univariate spline functions and $2K^2$ transformation parameters (8 bits each in 64-bit floating point). Furthermore, constructing F only requires updating two quantities for each location m and potentially interfered-with sector k'. Thus we have an F function that is efficient in terms of both space and run time, the resulting solutions to $x = F(x)$ closely match those for the F from Section 3 which is based on a spline approximation to the smoothed sawtooth from Section 2. In other words, we have an efficient version of F that is well motivated by time-average models of log-normal random variations.

As with our other modeling work motivated by practical optimization of wireless systems [6, 7, 8], we have seen that useful predictions can be made by efficient computational models that do not resort to simulation.

References

[1] W.-J. Oh and K. M. Wasserman, "Optimality of greedy power control and variable spreading gain in multi-class CDMA mobile networks," in *Proc. of*

the 5th Annual ACM/IEEE Int. Conf. on Mobile Computing and Networking, 1999, pp. 102–112.

[2] J. S. Lee and L. E. Miller, *CDMA Systems Engineering Handbook*. Artech House, 1998.

[3] S. Kandukuri and S. Boyd, "Optimal power control in interference-limited fading wireless channels with outage-probability specifications," *IEEE Trans. Wireless Commun.*, vol. 1, no. 1, pp. 46–55, Jan. 2002.

[4] R. D. Yates, "A framework for uplink power control in cellular radio systems," *IEEE J. Sel. Areas in Commun.*, vol. 13, no. 7, pp. 1341–1347, Sept. 1995.

[5] C. Nuzman, "Note on convergence of a non-monotonic power control model," 2006, private communication.

[6] K. L. Clarkson and J. D. Hobby, "A model of soft handoff under dynamic shadow fading," in *VTC-2004-Spring: IEEE Vehicular Technology Conference*, vol. 3, 2004, pp. 1534–1538.

[7] ——, "A model of coverage probability under shadow fading," 2003, to appear. [Online]. Available: http://cm.bell-labs.com/cm/cs/who/clarkson/covprob/p.pdf

[8] ——, "Ocelot's knapsack calculations for modeling power amplifier and walsh code limits," 2006, to appear. [Online]. Available: http://cm.bell-labs.com/cm/cs/who/hobby/lossmodel.pdf